Eur. J. Mineral.
2007, **19**, 871–882
Published online November 2007

Petrology of local concentration of chromian spinel in dunite from the slow-spreading Southwest Indian Ridge

TOMOAKI MORISHITA[1,*], JINICHIRO MAEDA[2], SUMIO MIYASHITA[3], HIDENORI KUMAGAI[4], TAKESHI MATSUMOTO[5] and HENRY J.B. DICK[6]

[1] Frontier Science Organization, Kanazawa University, Kanazawa 920-1192, Japan, and CNR-Istituto di Geoscienze e Georisorse Sezione di Pavia, via Ferrata, 1, 27100, Pavia, Italy
*Corresponding author, e-mail: moripta@kenroku.kanazawa-u.a.jp
[2] Graduate School of Science, Hokkaido University, Hokkaido 060-0810, Japan
[3] Department of Geology, Faculty of Science, Niigata University, Niigata 950-2181, Japan
[4] Japan Agency for Marine-Earth Science and Technology, Yokosuka 237-0061, Japan
[5] Physics and Earth Sciences, Faculty of Science, University of the Ryukyus, Okinawa 903-0213, Japan
[6] Department of Geology and Geophysics, Woods Hole Oceanographic Institution, Woods Hole 02543, USA

Abstract: This is the first detailed report on local concentration of chromian spinel in a dunite from an ultraslow spreading ridge, the Southwest Indian Ridge (SWIR). The sample was collected from an outcrop with detailed observations using submersible SHINKAI 6500 of the Japanese Marine Science Technology Center. The dunite occurs as a tabular-shaped layer in a lherzolite host outcrop. Spinel is found as a string of small micropods 2–3 centimeters in size. These spinel micropods make a layer in the middle part of a spinel-poor dunite (< 1 vol % spinel) parallel to the lithological boundary between dunite and enstatite-poor harzburgite. The enstatite-poor harzburgite has relatively high-Cr# spinel (> 0.4) compared with other peridotite samples in the studied area (lherzolites to harzburgite with low-Cr# spinel, typically Cr# $\leqslant$ 0.3). The occurrence and chemical compositions of clinopyroxene in the enstatite-poor harzburgite suggest that some clinopyroxenes crystallized from infiltrated interstitial melts. The host peridotites are interpreted as a residue of relatively low degrees of partial melting consistent with a location along the SWIR far from a mantle hot spot. This was then followed by crystallization of clinopyroxene from interstitial melt in the dunite. Irrespective of their small size, the lithological relationships between the spinel micropods and the host peridotites are the same as those for podiform chromitite in ophiolites and orogenic peridotites. The spinel Cr# in the micropods (0.3) is compatible with the lower range of those in basalts from SWIR far from hot spot. The spinel micropods were mainly formed by interaction between relatively depleted peridotite and a locally significant volume of basaltic melt traversing the upper mantle. This study coupled with the previous works on chromitites suggest that podiform chromites occur in every geodynamic setting, though economic concentrations of chromite (Cr-rich spinel) are unlikely to occur in the mantle at ultraslow spreading ridges.

Key-words: spinel, chromitite, dunite, slow-spreading ocean-ridge, ocean floor, melt-mantle interaction.

Introduction

Chromian spinel-rich rocks, *i.e.* chromitites, are commonly found as lenticular or pod-shaped bodies within tabular to irregular shaped dunite bodies, termed podiform dunite, enclosed in mantle tectonite peridotites in many ophiolites and orogenic peridotite massifs. They are called podiform chromitite (*e.g.*, Thayer, 1964) and have been mined as both a source of chrome and high alumina refractories. Chromitites appear to form by selective crystallization of chromian spinel from melts for a period of time and/or by selective concentration of chromite due to physical mechanisms such as flow differentiation and/or metamorphic differentiation (*e.g.*, Lago *et al.*, 1982; Leblanc & Ceuleneer, 1992). Chromian spinel is, however, a minor phase produced during closed-system cotectic crystallization of basaltic magmas (*e.g.*, Campbell & Murck, 1993). Edwards *et al.* (2000) suggested that the water content of basaltic melt plays a significant role in the formation of podiform chromitites as hydrous melts have a greater abundance of octahedral sites, which would promote greater chrome solubility. Irvine (1975, 1977) proposed that mixing of Si-rich and primitive basaltic melts would drive melts into the chromite phase field leading to formation of layered stratiform chromitite, another type of chromitite associated with large layered intrusions. This model can

DOI: 10.1127/0935-1221/2007/0019-1773
0935-1221/07/0019-1773 $ 5.40

be basically applied for the origin of podiform chromitites (Dick & Bullen, 1984; Arai & Yurimoto, 1994; Zhou *et al.*, 1994).

It is generally accepted that Si-rich secondary melts can be produced locally in mantle peridotites by reaction between the primitive basaltic melts and peridotites due to dissolution of pyroxene and precipitation of olivine during melt-rock reaction (*e.g.*, Dick, 1974; Kelemen, 1990). Where (or when) the melt supply is high, such Si-rich secondary melts can subsequently mix with more primitive basaltic magma in melt transport conduits. The origin of podiform chromitites is thus generally explained by crystallization from a hybridized melt because the mixed magma is expected to be oversaturated with chromite (*e.g.*, Arai & Yurimoto, 1994; Zhou *et al.*, 1994).

Field and geochemical evidence suggests that melt-mantle interactions are common in the upper mantle. Podiform chromitites are, however, more commonly found in harzburgite-dominated ophiolite and orogenic peridotites than in lherzolite-dominated ophiolite and orogenic peridotites (Boudier & Nicolas, 1985; Noller & Crater, 1986; Leblanc & Temagoult, 1989; Nicolas & Al Azri, 1991; Roberts & Neary, 1993). Dunite crosscutting layering and/or foliation plane of the host peridotites is commonly documented in the mantle sections and is interpreted to be a result of melt-rock interactions (*e.g.*, Dick, 1976; 1977a, b; Dick & Sinton, 1979; Quick, 1981; Piccardo *et al.*, 2007). The crosscutting dunites are not always associated with chromitites (Quick, 1981; Nicolas & Al Azri, 1991). Even if podiform chromitite exists in lherzolite-dominant ophiolite and orogenic peridotites, it is usually found closely associated with harzburgite (Zhou *et al.*, 1996; Morishita *et al.*, 2006).

Although podiform chromitites are common in supra-subduction zone mantle environments represented by ophiolites, their occurrence in other tectonic settings is still in debate (Roberts, 1988; Yumul, 1992; Arai, 1995, 1998, Arai & Yurimoto, 1995; Prichard *et al.*, 1996; Robinson *et al.*, 1997; Schiano *et al.*, 1997; Zhou & Robinson, 1997; Zhou *et al.*, 1998). This is partly because few chromitites have been collected from well-constrained tectonic settings. Several authors have suggested that major oceanic ridges are unlikely places for chromite mineralization to take place (Roberts, 1992; Zhou & Robinson, 1997; Arai, 1997a). Most abyssal peridotites, however, have been sampled at transform faults far from regions where focused melt flow likely occurs in the shallow mantle beneath ocean ridges (Dick, 1989). The average abyssal peridotite is close to harzburgite, while dunite, away from transform faults at the Gakkel, Southwest Indian Ridge and Mid-Atlantic Ridges, constitutes from 4 to 10 % of all peridotite sampled, and commonly contains small chromitite segregations, suggesting that podiform chromitites may be common in the shallow abyssal mantle at all spreading rates (Dick, Tivery & Tucholke, G3, in revision).

We report here the first detailed description of the petrology and geochemistry of a small dunite spinel segregation and host peridotite sampled from an ultraslow spreading ocean ridge representing a key end-member for seafloor spreading, crustal accretion and magma genesis. The sample, from the Atlantis II Fracture Zone at the Southwest Indian Ridge, despite its small size, effectively mirrors the formation of podiform dunites and chromitites commonly found in ophiolite peridotite massifs.

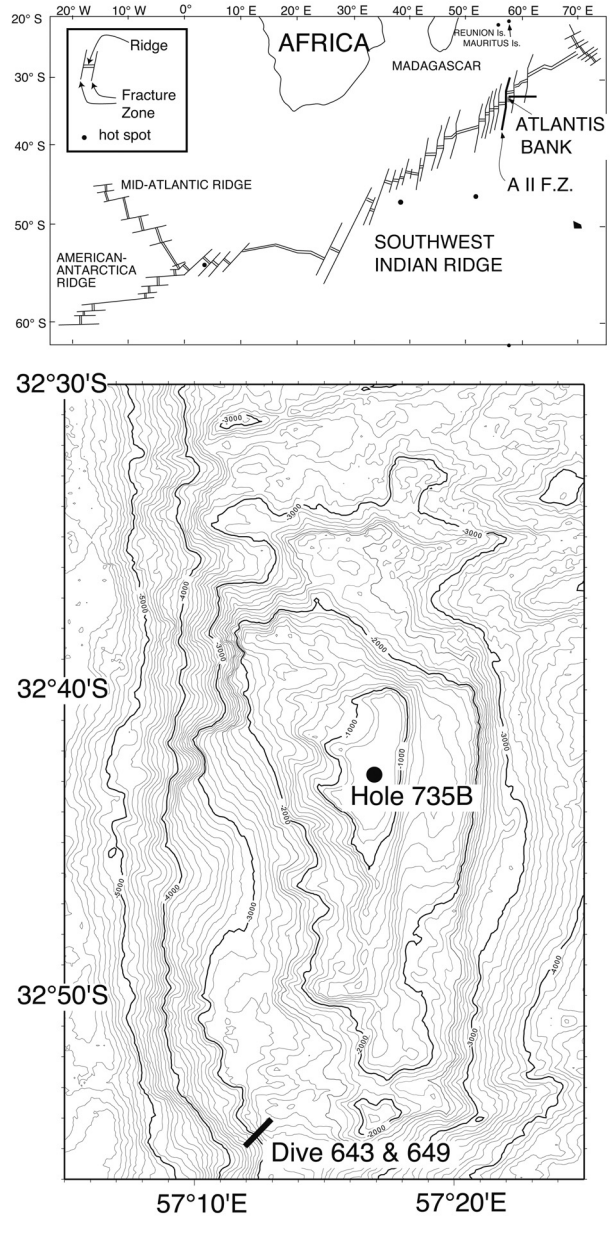

Fig. 1. (a) Location of the studied area on the Southwest Indian Ridge. Bathymetric map of the Atlantis Bank region adjacent to the Atlantis II Fracture Zone. Dives trace of No. 643 and No. 649 is the location from which the studied sample was collected. The site Hole 735B of the Ocean Drilling Program is also shown.

Geological background and sample description

The Southwest Indian Ridge (SWIR) is an ultraslow spreading ridge with a 14 mm/year full-spreading rate (Hosford *et al.*, 2003). The Atlantis II Fracture Zone is a

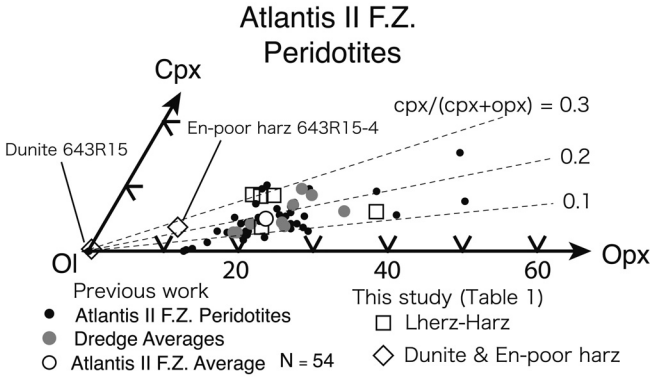

Fig. 2. Modal ternary diagram: clinopyroxene (Cpx)-olivine (Ol)-orthopyroxene (Opx) of the studied area with the compositions of the previous work from the Atlantis II Fracture Zone (Dick *et al.*, 1984; Johnson & Dick, 1992; Dick, H.J.B., unpublished data). En-p harz = Enstatite-poor harzburgite, Harz = harzburgite, Lherz = Lherzolite.

transform-valley, a 199 km offset of the SWIR (Fig. 1). Hole 735B of the Ocean Drilling Program (Legs 118 and 176) succeeded in recovering 1.5 km section of gabbroic rocks at Atlantis Bank which is located 100 km south of the SWIR rift valley on the crest of the eastern traverse ridge of the Atlantis II Fracture Zone (*e.g.*, Dick *et al.*, 2000) (Fig. 1).

Many peridotite samples were collected from outcrops exposed on the eastern rift valley wall of the Atlantis II Fracture Zone by the ABCDE cruise of the Japan Marine Science Technology Center (JAMSTEC) using submersible SHINKAI 6500 (Fig. 1). Dive 643 collected only peridotites from outcrops or on outcrops from 3396 m to 2564 m depth, whereas other 5 peridotites and 2 gabbros were collected from recent talus. Another dive (no. 649), which was conducted along an extended track from Dive 643, confirmed that gabbros are only exposed of 2561-2493 m depth. Accordingly, we describe only samples collected from outcrops and on outcrops (Table 1). Ten of 13 samples are lherzolite, two samples are clinopyroxene-bearing harzburgite (643R06, 643R07) and one is dunite (643R15) (Fig. 2). These indicate that mainly fertile peridotites crop out along the dive track, consistent with a slow-spreading ridge where degree of partial melting is expected to be relatively low often leaving lherzolite or clinopyroxene-rich harzburgite residues.

Dunite 643R15, the focus of this paper, has a distinctive ~ 1 cm spinel-rich layer a few centimeters in size with numerous aligned small irregular micropods of spinel. The dunite has a contact with a clinopyroxene-rich harzburgite (Enstatite-poor harzburgite hereafter) (643R15-4 in Table 1) roughly parallel to the spinel-rich layer at the edge of the sample (Fig. 3). Olivine textures in the dunite are masked by extensive serpentinization and alternation while, based on pyroxene morphology, the Enstatite-poor harzburgite has a protogranular texture. As the dunite is in contact with the harzburgite and occurs in an outcrop with massive granular peridotite, it is likely a crosscutting tabular body typical of many dunites in mantle peridotites. A

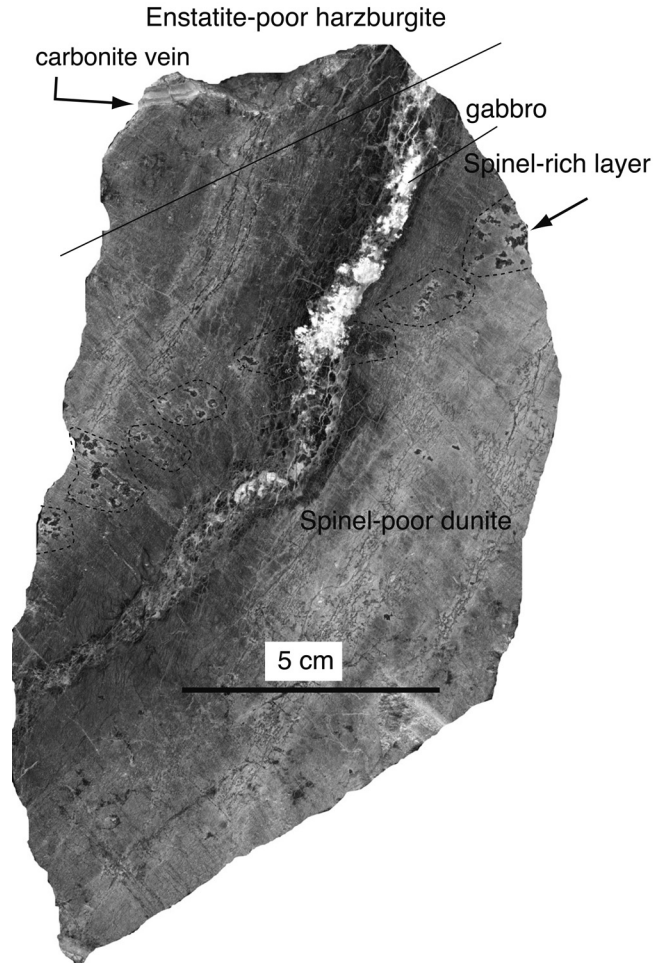

Fig. 3. Sawed surface of the sample with spinel-rich layer. Note that several spinel-rich micropods (surrounded by broken line) make a layer concordant with lithological boundary between dunite and Enstatite-poor harzburgite.

~ 1–1.5 cm gabbro vein also cuts irregularly through the sample, crosscutting the spinel-rich layer (Fig. 3) with a sharp contact with dunite (Morishita *et al.*, 2004), representing a late intrusion crystallized from basaltic melt. The gabbro vein contains a small amount of titanium and/or zirconium oxide minerals such as rutile, ilmenite, zircon and srilankite (Morishita *et al.*, 2004). Although the gabbroic vein is extensively altered, anhedral granular-shaped orthopyroxene is the main primary igneous phase remaining. Some orthopyroxenes in the gabbro vein, however, are interpreted to be formed by reaction between SiO_2-component in the melts and olivine in the peridotite hosts (Morishita *et al.*, 2004). Many carbonate veins ranging from a few millimeters to a centimeter in thickness then cut all lithologies.

The dunite mainly consists of olivine (now completely serpentinized and/or altered) with minor amount of spinel and clinopyroxene. Clinopyroxene usually occurs with spinel as a symplectitic mineral aggregate (cpx-spl symplectite hereafter) (Fig. 4a). Only a minor amount of very fine-grained clinopyroxene (< 30 μm) is found as isolated

Table 1. Locations, Depths and mineral modes of the samples. Primary modes were reconstructed by point-counting for each sample from several thin sections (N represents numbers of thin sections we analyzed), except for 643R15-4, in 500 μm × 500 μm grid. Although the degree of serpentinization is generally high, serpentine and alteration products (except for carbonate) are counted as the pseudomorph of each phase (*i.e.*, olivine, orthopyroxene, clinopyroxene, spinel). A correction for volume expansion during alteration was not applied. All point counts were performed by the first author. 643R15-4* = Enstatite-poor harzburgite part of 643R15 (En-p harz). Lat. = latitude, Log. = longitude, Lherz = lherzolite, Harz = harzburgite, GB = gabbro vein, Cr = spinel concentration, CPX = clinopyroxenite vein, N = numbers of thin sections analyzed for modal counts, ol = olivine/ (total counts-carbonate counts), opx = orthopyroxene/ (total counts-carbonate counts), cpx = clinopyroxene/ (total counts-carbonate counts), spl = spinel/ (total counts-carbonate counts), Cpx% = clinopyroxene/(clinopyroxene + orthopyroxene), Alt % = (serpentine + alteration product counts)/(total counts-carbonate counts), Carb% = carbonate counts/total counts.

sample name	depth (m)	occurrence	type	remark	N	ol	opx	cpx	spl	Cpx %	Alt %	Carb%
643R01	3396	outcrop	Lherz		3	74 (6)	17 (1)	9 (5)	< 1	34 (15)	85 (3)	0
643R02	3396	outcrop	Lherz									
643R03	3281	outcrop	Lherz									
643R04	3276	outcrop	Lherz									
643R06	2974	on outcrop	cpx Harz		3	75 (5)	21 (3)	3 (2)	< 1	11 (6)	60 (1)	0
643R07	2974	on outcrop	Harz	GB								
643R14	2622	outcrop	Lherz		2	73 (0.2)	18 (1)	9 (2)	< 1	34 (6)		
643R15	2605	outcrop	Dun	Cr, GB	3	99 (0.02)	0	< 1	< 1	-	99 (0.1)	16 (10)
643R15-4*	2605	outcrop	Dun lherz		1	87	10	3	< 1	25	93	13
649R01	2609	outcrop	Lherz									
649R02	2609	outcrop	Lherz	CPX								
649R03	2593	outcrop	Lherz		2	59 (2)	34 (2)	6 (4)	< 1	13 (8)	87 (4)	34 (4)
649R04	2577	outcrop	Lherz									
643R05	2564	outcrop	Lherz		3	71 (6)	19 (7)	9 (2)	< 1	32 (13)	77 (5)	34 (8)

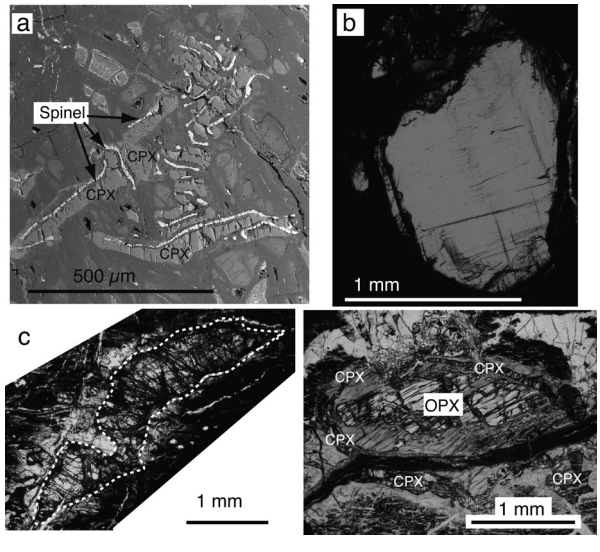

Fig. 4. Variations in clinopyroxene occurrences from dunite and enstatite-poor harzburgite. (a) Back scattered electron image of symplectitic mineral aggregate of spinel and clinopyroxene in the dunit. (b) Photomicrograph of discrete grain in Estatite-poor harzburgite. Plane-polarized light. (c) Photomicrograph of interstitial grain in Enstatite-poor harzburgite. Plane-polarized light. (d) Photomicrograph of rimming of orthopyroxene porphyroclast in Enstatite-poor harzburgite. Plane-polarized light.

grains in olivine matrix. Rounded anhedral spinel also occurs as discrete grains (< 5 mm across). The dunite, excluding the spinel-rich layer, is spinel-poor (< 1 vol %) (Table 1). Mineral inclusions in the spinel (*e.g.*, pyroxenes, pargasite and phlogopite), which are common in ophiolites and orogenic peridotites (*e.g.*, Johan *et al.*, 1980; Talkington *et al.*, 1986; Augé, 1987; Lorand & Ceuleneer, 1989; McElduff & Stupfl, 1991; Matsumoto *et al.*, 1995; Schiano *et al.*, 1997; Matsukage & Arai, 1998; Ahmed & Arai, 2002, Morishita *et al.*, 2006), were not found. The protogranular Enstatite-poor harzburgite at the contact consists of olivine with small amount of pyroxenes and spinel. However, cpx/(cpx+opx) ratio is high similar to the other typical lherzolites (Fig. 2). Clinopyroxene in the Enstatite-poor harzburgite has several modes of occurrence; coarse discrete grain (Fig. 4b), interstitial grain (Fig. 4c) and rimming of large orthopyroxene grain (Fig. 4d) (referred to as discrete, interstitial and rimming clinopyroxenes hereafter). This textural variability likely indicates multiple origins as discussed below.

Other peridotite samples collected from the same dive sites have also undergone variable degrees of serpentinization and/or alteration, but have protogranular to weak porphyroclastic textures. Some peridotites are intruded by gabbroic vein (643R07) or clinopyroxenite (649R02).

Mineral chemistry

Major-element compositions of minerals were determined with a JEOL JXA-8800 Superprobe at the Center for Cooperative Research of Kanazawa University. The analyses were performed with an accelerating voltage of 15–20 kV and a beam current of 15–20 nA using a 3 μm diameter beam. Details of the analysis are shown in Morishita *et al.*, (2004). Spinel and clinopyroxene in the dunite near the gabbro vein have a distinctively TiO_2-enriched character compared to those far from the gabbro vein (Fig. 5) (Morishita *et al.*, 2004). The mineralogy of the gabbros suggests that the TiO_2-rich melt was required for the formation of the gabbro. However ilmenite grains in the gabbro vein are distinctively high in MgO compared with those in both oxide-poor olivine gabbros and Fe-Ti-rich oxide gabbros collected from the studied area (Bloomer *et al.*, 1989; Dick *et al.*, 2000). Furthermore, the Cr_2O_3 content in rutile in the gabbro vein is also high. Based on these features,

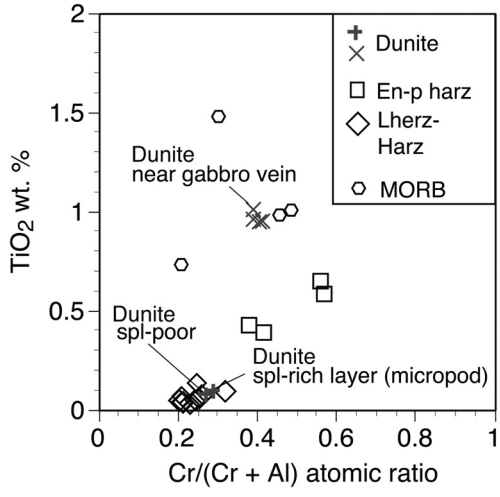

Fig. 5. Compositional relationship between Cr# (= Cr/(Cr + Al) atomic ratio) and TiO_2 wt. % of spinels in the studied dive sites. Data of chromite grains in MORB from the Southwest Indian Ridge are from le Roex *et al.*, (1983). Those in dunite near the gabbro vein are from Morishita *et al.*, (2004).

Morishita *et al.*, (2004) suggested that the gabbroic vein was formed from an in-situ highly fractionated melt from a MORB-type melt during ascent in the upper mantle. The TiO_2-enriched minerals would result from the interaction with the TiO_2-rich fractionated melts responsible for the formation of the gabbro vein after the formation of spinel-rich layer. In order to avoid the metasomatic effects of the TiO_2-rich melts on samples, we basically discuss chemical characteristics of minerals far from the gabbro vein. It is, however, difficult to completely avoid the metasomatic effects of the TiO_2-rich melts because of the size of the sample.

Dunite

There are no apparent differences in the chemistry of spinel between spinel-rich layer and discrete grains in the dunite except for Mg# (Table 2). The Cr# and TiO_2 contents of spinel are 0.3 and 0.1 wt. %, respectively (Fig. 5 and 6). Those of spinel near gabbro reach 0.5 and 1.5 wt. %, respectively (Morishita *et al.*, 2004) (Fig. 5 and 6). The Mg# of chromite is 0.74 and 0.70 for spinel-rich layer and discrete grain in dunite, respectively. The chemical compositions of clinopyroxene are different reflecting the differences in occurrences. The symplectite clinopyroxenes are higher in the Cr_2O_3 and Na_2O contents (1 and 0.6 wt. %, respectively) than discrete clinopyroxenes (0.2–0.4 and < 0.3 wt. %, respectively) (Fig. 7 and Table 2).

Enstatite-poor harzburgite

The chemical compositions of spinel in the Enstatite-poor harzburgite 643R15-4 have variations in the Cr# and TiO_2 contents ranging from 0.4 to 0.6, and from 0.1 to 0.7 wt. %, respectively (Fig. 5 and 6). The high Cr# spinel is also high in TiO_2 content. These grains were also affected by interaction with the TiO_2-rich melt for the formation of the gabbro vein. The chemical compositions of clinopyroxene between discrete grains and interstitial grains are similar to each other in the core, whereas those of rimming grains are slightly different from the former two types. The Al_2O_3 and Na_2O contents are lower and higher in the rimming clinopyroxene than in the other two clinopyroxenes (Fig. 7 and Table 2). The Al_2O_3, Cr_2O_3 and TiO_2 contents of the core of orthopyroxene porphyroclast are 3.5, 0.5 and 0.1 wt. %, respectively (Table 2).

Other peridotites

The spinel Cr# in the remaining peridotites collected from the same dive sites ranges from 0.2 to 0.35, mostly around 0.2 (Fig. 6), except 643R07 (0.4–0.6) which has a gabbroic vein. Spinel TiO_2 contents are low, < 0.1 wt. %, except 643R07 (0.4–0.8 wt. %). The peridotite spinel chemical compositions (except 643R07) are consistent with those in mantle residue of a low-degree of partial melting predicted for slow-spreading ridges (Dick & Bullen, 1984; Arai, 1994a,b). The forsterite content of olivine is 90 in lherzolite and 91 in harzburgite (Table 5). The Al_2O_3, Cr_2O_3 and Na_2O contents of the core of clinopyroxene porphyroclast are 6–7 wt. %, < 1.3 wt.%, and < 0.3 wt. % in lherzolite, and 5, 8, and 0.6 wt. % in harzburgite, respectively (Fig. 7 and Table 5). The Al_2O_3, Cr_2O_3 and TiO_2 contents of enstatite porphyroclast cores are 5, 1 and < 0.04 wt. % respectively in lherzolite, and 4, 1 and 0.1 wt. % in harzburgite (Table 5).

Discussion

Origin of the Enstatite-poor harzburgite

Mineral textures in the peridotites are typical of granular peridotites emplaced by solid-state flow to the base of the crust at ocean ridges, and these rocks appear little affected by higher-grade ductile deformation associated with detachment faulting and emplacement seen elsewhere. In particular, the dunite crosscuts these peridotites, and the spinels are irregular aggregates that show little visible evidence of deformation. Thus, the layering consisting of the spinel micropod layer, spinel-poor dunite and the adjoing Enstatite-poor harzburgite are a primary magmatic feature rather than a mechanical accumulation of minerals due to physical mechanisms such as flow differentiation and/or metamorphic differentiation.

Atlantis II transform residual peridotite spinel compositions have a limited local variation with low Cr# in residual mantle rocks (Dick, 1989; Johnson & Dick, 1992). The previous study on abyssal peridotites suggests that spinel Cr# is a good indicator for the degree of partial melting of plagioclase-free-and vein-free peridotitic residues (Dick & Bullen, 1984; Arai, 1987; Hellebrand *et al.*, 2001). The fertility of most SWIR peridotite away from mantle

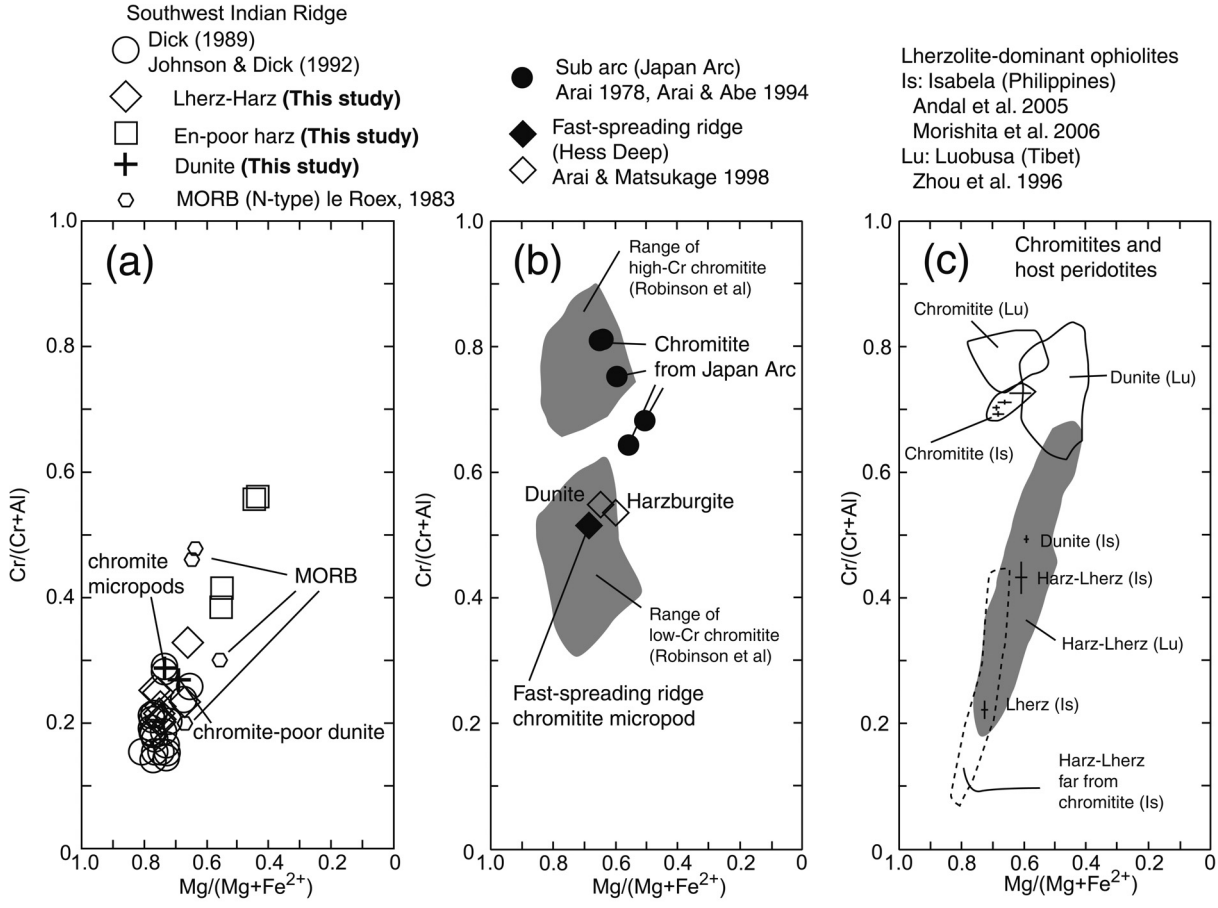

Fig. 6. Compositional relationship between Mg# (= Mg/(Mg + Fe^{2+}) atomic ratio) and Cr# (= Cr/(Cr + Al) atomic ratio) of spinel. (a) Studied samples including peridotites collected from the Southwest Indian Ridge far from hot spots by Dick (1989) and Johnson & Dick (1992). (b) Chromitite xenoliths in alkaline basalt magmas from Japan Arc (Arai, 1978; Arai & Abe, 1994) and Oceanic chromitites from a first-spreading ridge (Arai & Matsukage, 1998). The compositional ranges of high-Cr and low-Cr chromitites (Robinson *et al.*, 1997) are also shown. (c) Podiform chromitites in two lherzolite-dominant ophiolites: The Luobusa ophiolite (Zhou *et al.*, 1996) and the Isabela ophiolite (Andal *et al.*, 2005). Data of peridotites far from chromitites and chromitites with host peridottes are from Andal *et al.*, (2005) and Morishita *et al.*, (2006), respectively.

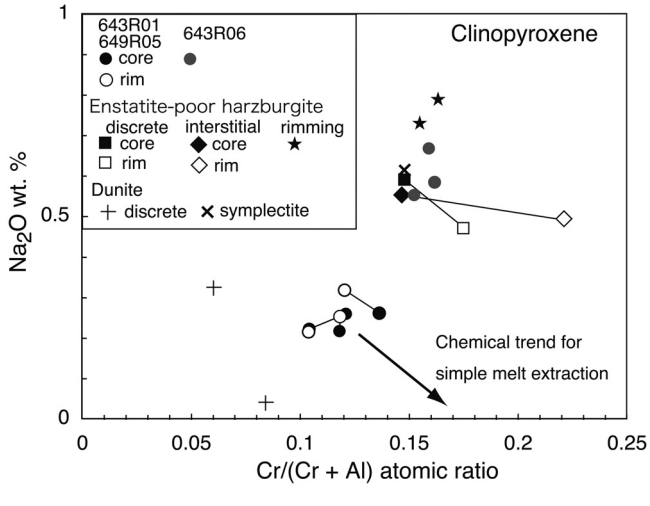

Fig. 7. Compositional relationship between Cr# (Cr/(Cr+Al) atomic ratio) and Na_2O wt. % of clinopyroxenes in the dunite, Enstatite-poor harzburgite and other peridotites in the studied area.

hotspots is the result of the slow spreading rate combined with the cooling effect of the transform faults (Hellebrand *et al.*, 2002). Locally, however, spinel in the Enstatite-poor harzburgite is relatively high (Cr# = 0.4–0.6) compared with those in other peridotites collected from the same site (this study) as well as previous work from the Atlantis II Fracture Zone (Dick, 1989; Johnson & Dick 1992) (Cr# = 0.15*–0.35) (Fig. 6). Higher spinel Cr# generally correlates well with depletion and inferred degree of mantle melting in abyssal peridotites (Dick & Bullen, 1984; Dick *et al.*, 1984; Hellebrand *et al.*, 2002). On the other hand, TiO_2 and Na_2O contents of clinopyroxene in the Enstatite-poor harzburgite are all higher than predicted by partial melting (Fig. 7). This combined with textural observations on clinopyroxene suggests that some or most of clinopyroxene in the Enstatite-poor harzburgite might be not a simple residual origin but have partially re-equilibrated with later infiltrating MORB melt. Similar crystallization of clinopyroxene from infiltrating interstitial melt has been found for other slow-spreading ridge peridotites (Seyler *et al.*, 2001).

Table 2. Major-element compositions of minerals in dunite including chromite-rich layer. CPX = clinopyroxene, OPX = orthopyroxene, Dis = discrete grain, Symp = symplectitic aggregate, vein = spinel-rich vein in dunite, AV = average, STD = standard deviation, Numbers in parenthesis next to the STD = numbers of analysis.

Mineral	CPX				Spinel			
Occurrence	Dis	Dis	Symp		vein		Dis	
			Av	STD (5)	Av	STD (7)	Av	STD (7)
wt. %								
SiO_2	51.2	54.0	52.0	0.20	< 0.04		< 0.04	
TiO_2	0.47	0.21	0.24	0.01	0.10	0.03	0.08	0.03
Al_2O_3	3.8	1.4	4.4	0.32	41.3	0.49	41.9	0.77
Cr_2O_3	0.36	0.19	1.13	0.08	25.3	0.32	23.3	1.27
FeO	2.7	1.5	2.5	0.23	14.9	0.71	16.9	0.72
MnO	< 0.07	< 0.07	< 0.07		0.18	0.04	0.15	0.05
MgO	15.9	17.5	15.6	0.25	17.7	0.24	16.7	0.69
CaO	25.2	25.9	24.2	0.41	< 0.04		< 0.04	
Na_2O	0.33	< 0.04	0.61	0.05	< 0.04		< 0.04	
K_2O	< 0.03	< 0.03	< 0.03		< 0.03		< 0.03	
NiO	n.a.	n.a.	< 0.05		n.a.		n.a.	
total	100.0	100.7	100.7	0.28	99.5	0.82	99.1	1.05
Numbers of cations on the basis of O=6 for pyroxenes and O=4 for spinel								
O=	6	6	6		4		4	
Si	1.88	1.95	1.89	0.01				
Ti	0.01	0.01	0.01	0.00	0.00	0.00	0.00	0.00
Al	0.16	0.06	0.19	0.01	1.37	0.01	1.40	0.03
Cr	0.01	0.01	0.03	0.00	0.56	0.00	0.52	0.03
Fe*	0.08	0.05	0.08	0.01	0.35	0.02	0.40	0.02
Mn			0.00	0.00	0.00	0.00	0.00	0.00
Mg	0.87	0.94	0.84	0.01	0.74	0.01	0.70	0.02
Ca	0.99	1.00	0.94	0.02				
Na	0.02		0.04	0.00				
K								
Ni								
total	4.03	4.01	4.02	0.00	3.03	0.00	3.03	0.01
Mg#	0.913	0.953	0.918	0.007	0.735	0.011	0.696	0.023
Cr#	0.060	0.084	0.148	0.002	0.291	0.002	0.272	0.014
Y Fe3+					4.1	0.6	4.7	0.6
Y Al					67.9	0.5	69.4	1.8
Y Cr					27.9	0.3	25.9	1.2

Furthermore, higher Na_2O and TiO_2 contents of rimming clinopyroxene were probably locally formed by the high-TiO_2 melt for the formation of the later gabbro vein. Some spinels with high Cr# was also probably affected by the high-TiO_2 melt. This would also explain the anomalously high cpx/(cpx+opx) ratio (Fig. 2). Intrusion of the gabbro vein was fracture controlled rather than due to large scale permeable flow, the influence of the melt producing the gabbro vein is limited to the immediate vicinity of the vein. Since low range of the Cr# of spinel in the Enstatite-poor harzburgite is still higher than the others at our dive site, then, could reflect higher degrees of melting than elsewhere along the Atlantis II Transform. In conclusion, the Enstatite-poor harzburgite is interpreted to be a partial melting residue later infiltrated by a MORB-like melt and the TiO_2-rich melt for the formation of the gabbro vein. Although little shallow melt transport is generally expected near transforms due to focusing of melt flow towards the mid-point of the adjoining magmatic segment (Dick, 1989), dunite is generally accepted as the product of melt-rock reaction stripping pyroxene from the host peridotite by ascending melt in a zone of focused flow (*e.g.*, Dick, 1976a; Quick, 1981; Nicolas, 1989; Kelemen, 1990). Thus, it is clear that at least some melt was transported through the shallow mantle beneath the transform zone at the Atlantis II Fracture Zone.

Origin of the spinel micropods in slow-spreading ridge dunites

It should be emphasized that the spinel-rich layer consists of several spinel micropods within spinel-poor dunite matrix (Fig. 3). Irrespective of its small size, the spinel-rich layer shares the same petrographical characteristics with podiform chromitites in ophiolites and orogenic peridotites as the product of late channelized melt transport and melt-rock reaction in the shallow mantle.

Table 3. Major-element compositions of minerals in dunitic lherzolite. CPX = clinopyroxene, OPX = orthopyroxene, Dis = discrete grain, Int = interstitial grain, Porph = porphyroclastic grain.

Mineral	CPX					OPX			Spinel	
Occurrence	Dis core	Dis rim	Int core	Int rim	Rim	Rim	Porph core	Porph rim		
wt. %										
SiO_2	51.5	52.5	51.0	52.6	52.1	52.1	55.8	56.7	< 0.04	0.08
TiO_2	0.16	0.18	0.17	0.18	0.21	0.23	0.08	0.10	0.44	0.65
Al_2O_3	5.5	3.7	5.5	2.6	4.4	4.3	3.5	2.8	33.7	22.1
Cr_2O_3	1.4	1.2	1.4	1.1	1.3	1.2	0.51	0.70	31.1	42.3
FeO	2.7	2.8	3.0	2.6	3.4	3.4	7.7	7.4	20.8	24.4
MnO	0.10	0.08	0.11	0.10	0.12	0.12	0.14	0.18	0.25	0.36
MgO	15.0	16.7	16.3	16.6	15.7	16.0	32.4	32.9	12.9	9.3
CaO	22.3	22.4	21.0	22.7	21.4	21.1	0.87	0.90	< 0.04	< 0.04
Na_2O	0.59	0.47	0.55	0.49	0.79	0.73	< 0.04	< 0.04	< 0.04	< 0.04
K_2O	< 0.03	< 0.03	< 0.03	< 0.03	< 0.03	< 0.03	< 0.03	< 0.03	< 0.03	< 0.03
NiO	0.05	0.05	< 0.05	0.05	< 0.05	0.04	0.07	0.08	0.16	0.08
total	99.3	100.0	99.3	99.1	99.6	99.1	101.1	101.7	99.4	99.3
Numbers of cations on the basis of O=6 for pyroxenes and O=4 for spinel										
O=	6	6	6	6	6	6	6	6	4	4
Si	1.89	1.91	1.87	1.93	1.91	1.91	1.92	1.94		
Ti	0.004	0.005	0.005	0.005	0.006	0.006	0.002	0.003	0.010	0.016
Al	0.24	0.16	0.24	0.11	0.19	0.19	0.14	0.11	1.18	0.83
Cr	0.042	0.033	0.041	0.032	0.037	0.034	0.014	0.019	0.732	1.069
Fe	0.083	0.086	0.093	0.080	0.10	0.10	0.22	0.21	0.52	0.65
Mn	0.003	0.002	0.003	0.003	0.004	0.004	0.004	0.005	0.006	0.010
Mg	0.82	0.90	0.89	0.91	0.86	0.87	1.66	1.67	0.57	0.45
Ca	0.87	0.87	0.83	0.90	0.84	0.83	0.032	0.033		
Na	0.042	0.033	0.039	0.035	0.056	0.052	0.002	0.002		
K										
Ni	0.002	0.001		0.001		0.001	0.002	0.002	0.004	0.002
total	3.99	4.01	4.01	4.01	4.00	4.00	4.00	4.00	3.03	3.03
Mg#	0.908	0.914	0.905	0.919	0.893	0.894	0.882	0.889	0.564	0.436
Cr#	0.148	0.174	0.146	0.221	0.162	0.155	0.089	0.144	0.382	0.562
Y Fe3+									3.9	3.9
Y Al									59.4	42.1
Y Cr									36.7	54.0

In contrast to the Enstatite-poor harzburgite, the spinel-poor dunite has little clinopyroxene and is nearly orthopyroxene-free. The boundary between the spinel-poor dunite and the Enstatite-poor harzburgite is sharp (Fig. 3). Spinel TiO_2 and Cr#, and discrete clinopyroxene TiO_2 and Na_2O contents in the dunite host are distinctively lower than that of the Enstatite-poor harzburgite (Fig. 5–7), but very similar to that found in remaining peridotites. These characteristics are typical of residual peridotites that have undergone fractional melting. The last melt increments produced during such melting are ultra-depleted with very low TiO_2, Na_2O and other incompatible elements (Dick & Natland, 1996). Thus, if the spinel-rich layer and dunite were originally the product of melt rock reaction with a MORB melt, they were subsequently modified by re-equilibration with an infiltrating ultra-depleted melt at the end of mantle melting. Physical evidence of the latter can be seen in the highly depleted composition of the discrete clinopyroxene in the dunite which likely crystallized from this cryptic melt.

When primitive basaltic melts generated by partial melting of peridotite migrate upward, they selectively react with orthopyroxene in peridotite wall-rock to produce SiO_2-rich secondary melts, resulting in the formation of a dunite (*e.g.*, Dick, 1974; 1976; Kelemen, 1990). While it is clear that a late ultra-depleted high silica melt was present at the end of melting (Sobolev & Shimizu, 1993), and infiltrated the dunite as well, this cannot by itself explain the spinel-rich layer with its concordant contact with the host peridotite. Thus, the present composition of the spinel-rich layer reflects this event, but its crystallization could likely have been triggered by mixing of the ultra-depleted melt with a primitive MORB melt in a dunite conduit. The permeability of dunite is higher than that of the host peridotite (Toramaru & Fujii, 1986; Zhu & Hirth, 2003), and thus during late stage melt transport ultra-depleted melt present in the host peridotite at the end of melting will be drawn into the conduit to mix with whatever melt is passing through, and may later entirely re-equilibrate with olivine and spinel in the conduit – erasing the initial mineral compositions signature of the original melt migrating through the dunite that produced it. The hybridized melt is formed by the mixing of primitive basaltic melts traversing the dunite conduit with the SiO_2-rich secondary melts drawn in from the host peridotite. This would likely draw the hybrid melt into the spinel stability field resulting in excess the local concern spinel precipitation and the local concentration of spinel in the micropods in this study, as suggested for the origin of chromitites (Irvine, 1975, 1977; Dick & Bullen, 1984; Arai & Yurimoto, 1994; Zhou *et al.*, 1994).

Table 4. Major-element compositions of spinel in lherzolite to harzburgite. STD = standard deviation, numbers in parenthesis next to the STD = numbers of analysis.

Sample	643R01-2	STD (7)	643R02	STD (6)	643R03	STD (11)	643R04	STD (7)	643R06	STD (11)	643R14	STD (11)	649R01	STD (7)	649R02	STD (6)	649R03	STD (9)	649R04	STD (11)	649R05	STD (9)
wt. %																						
TiO_2	0.04	0.02	0.07	0.02	0.05	0.02	0.14	0.03	0.10	0.02	0.05	0.01	0.06	0.02	0.08	0.02	0.04	0.02	0.05	0.02	0.03	0.02
Al_2O_3	47.9	0.4	48.0	0.8	47.8	1.3	44.8	0.7	39.4	1.5	47.9	1.6	44.6	0.4	44.0	1.0	48.1	0.9	45.2	0.8	46.5	0.9
Cr_2O_3	19.4	0.4	19.2	0.7	18.5	0.8	22.1	0.8	27.8	1.5	18.4	0.9	22.6	0.4	23.3	1.2	19.5	1.0	21.7	1.0	20.9	0.9
FeO	13.7	0.7	12.8	0.1	15.0	1.7	15.0	0.5	14.9	0.8	14.2	1.5	13.9	0.7	13.5	0.4	14.3	1.3	15.6	1.7	13.9	0.7
MnO	0.12	0.05	0.12	0.01	0.14	0.02	0.15	0.02	0.18	0.02	0.14	0.01	0.14	0.02	0.16	0.01	0.16	0.04	0.18	0.03	0.14	0.05
MgO	18.2	0.4	18.7	0.4	18.0	0.7	18.0	0.4	16.8	0.6	18.2	0.6	17.8	0.5	17.8	0.3	17.9	0.7	16.6	1.2	18.1	0.4
NiO	n.a.		0.27	0.01	0.29	0.02	0.25	0.02	0.21	0.01	0.26	0.03	0.22	0.02	0.24	0.02	n.a.	n.a.	0.24	0.02	n.a.	n.a.
total	99.4	0.8	99.2	1.1	99.9	0.7	100.4	0.6	99.5	0.7	99.3	0.3	99.4	0.3	99.2	0.2	100.0	0.9	99.5	1.0	99.6	0.9
Ti	0.001	0.000	0.001	0.000	0.001	0.000	0.003	0.001	0.002	0.000	0.001	0.000	0.001	0.000	0.002	0.000	0.001	0.000	0.001	0.000	0.001	0.000
Al	1.54	0.01	1.54	0.01	1.54	0.01	1.45	0.02	1.32	0.04	1.55	0.04	1.46	0.01	1.44	0.03	1.54	0.02	1.48	0.02	1.50	0.02
Cr	0.42	0.01	0.41	0.02	0.40	0.00	0.48	0.02	0.62	0.04	0.40	0.02	0.50	0.01	0.51	0.03	0.42	0.02	0.48	0.02	0.45	0.02
Fe	0.31	0.01	0.29	0.01	0.34	0.00	0.35	0.01	0.35	0.02	0.33	0.04	0.32	0.02	0.31	0.01	0.33	0.03	0.36	0.04	0.32	0.02
Mn	0.003	0.001	0.003	0.000	0.003	0.000	0.004	0.001	0.004	0.000	0.003	0.000	0.003	0.000	0.004	0.000	0.004	0.001	0.004	0.001	0.003	0.001
Mg	0.74	0.01	0.76	0.01	0.73	0.00	0.74	0.01	0.71	0.02	0.74	0.02	0.73	0.02	0.74	0.01	0.72	0.02	0.69	0.04	0.74	0.01
Ni			0.006	0.000			0.005	0.000	0.005	0.000	0.006	0.001	0.005	0.000	0.005	0.000	n.a.		0.005	0.000	n.a.	
total	3.02	0.00	3.02	0.00	3.02	0.02	3.03	0.00	3.02	0.00	3.02	0.01	3.02	0.00	3.02	0.00	3.02	0.00	3.02	0.00	3.02	0.00
Mg#	0.74	0.01	0.76	0.01	0.73	0.02	0.73	0.01	0.71	0.02	0.74	0.02	0.73	0.02	0.74	0.01	0.72	0.02	0.68	0.04	0.73	0.01
Cr#	0.21	0.00	0.21	0.01	0.21	0.01	0.25	0.01	0.32	0.02	0.20	0.01	0.25	0.00	0.26	0.01	0.21	0.01	0.24	0.01	0.23	0.01
YFe^{3+}	2.4	0.6	2.3	0.3	3.5	0.9	3.7	0.3	3.0	0.3	3.1	1.3	2.6	0.2	2.4	0.4	2.3	0.6	2.2	0.4	2.6	0.6
YAl	76.7	0.4	77.0	0.6	76.7	1.4	72.4	0.9	65.9	2.0	77.0	2.0	72.7	0.5	72.0	1.3	76.9	1.2	74.0	0.9	74.8	1.0
YCr	20.8	0.5	20.7	0.8	19.9	1.0	24.0	0.9	31.1	1.9	19.8	1.1	24.7	0.5	25.6	1.4	20.9	1.1	23.8	0.9	22.5	1.1

Arai (1997a, b) emphasized that the chemistry of the host peridotites controls the formation of podiform chromitites, particularly high-Cr and/or large chromitites in ophiolite/orogenic peridotites. Arai & Abe (1995) and Arai (1997a, b) suggested that moderately refractory harzburgite with intermediate Cr#-spinel (Cr# = 0.4–0.6) is the most suitable host for large-scale podiform chromitites because orthopyroxene in lherzolite is too low in Cr# to concentrate chromite (as opposed to more aluminous spinel) due to melt-peridotite interactions. In fact, even in lherzolite-dominant ophiolites and orogenic peridotites, podiform chromitite is usually found closely associated with harzburgite (Zhou *et al.*, 1996; Morishita *et al.*, 2006). In these cases, gradual lithological changes from dunites to lherzolites through harzburgite have been described around these chromitite pods (Zhou *et al.*, 1996; Morishita *et al.*, 2006). Given the similarity of the spinel in the dunite to that in the surrounding peridotites (excluding the Enstatite-poor harzburgite), we conclude that the studied spinel micropods were locally formed due to melt-peridotite interactions in a region and/or time with a relatively high rate of magma supply near the transform.

Implications for petrogenesis of podiform chromitites

Podiform chromitites are ubiquitous in podiform and tabular dunites found in orogenic and ophiolitic peridotites. They occur in deposits up to many thousands of tons of massive ore, and range down in size to micro-deposits such as we find in our dunite 643R15. Podiform chromitites include both high-alumina and high-chromium ore deposits, and are significant source of both chrome ore and high-alumina spinel furnace refractories. The Cr# in our spinel-rich clots, however, is lower than the large majority of podiform chromitites in ophiolites and orogenic peridotites (0.19–0.8) (Dick & Bullen, 1984; Arai, 1997a, b), the very few oceanic chromitites reported to date (0.5–0.6) (Arai & Matsukage, 1998), and chromitite xenoliths beneath Japan Arc (0.6–0.8) (Arai, 1978; Arai & Abe, 1994), and is similar to the lowest end of the low-Cr chromitites of Robinson *et al.*, (1997) (Fig. 6).

The range of spinel Cr# in our residual lherzolite and harzburgite is similar to that from the Isabela ophiolite in Philippines (Andal *et al.*, 2005) and overlap that of the Luobusa ophiolite in Tibet (Zhou *et al.*, 1997): both lherzolite-dominated ophiolites (Fig. 6). However, the Cr# of spinel in chromitites is much lower in our sample than in these chromitites from those ophiolites. These differences in spinel Cr# between them likely reflect the differences in the geochemical characteristics of melts responsible for the formation of chromitites.

Chrome generally has a very low solubility in basaltic melts, 330–520 ppm in MORB (Roeder & Reynolds, 1991). Water in melts may have a strong influence on increasing the solubility of Cr, however, because it will depolymerize the melt silica network (Edwards *et al.*, 2000). Hydrous silicate minerals such as amphibole and phlogopite within chromite are common in chromitite (Talkington *et al.*, 1986; Augé, 1987; McElduff & Stumpfl, 1991;

Table 5. Representative mineral compositions of lherzolite and harzburgite. STD = standard deviation, N = numbers of analysis, ol = olivine, cpx = clinopyroxene, opx = orthopyroxene, Mg# = Mg/(Mg+Fe^{total}) atomic ratio, Cr# = Cr/(Cr+Al) atomic ratio.

lithology	lherzolite		cpx-bearing harzburgite									lherzolite			
sample No.	643R01-2						643R06					649R05			
mineral	olivine	std	opx core	opx rim	cpx core	cpx rim	ol	std	opx core	opx rim	cpx	opx core	opx rim	cpx core	cpx rim
	N = 5						N = 6								
SiO_2	40.8	0.2	54.1	55.9	50.5	52.9	41.2	0.1	55.1	57.1	52.2	54.5	54.7	50.6	51.8
TiO_2	< 0.04		< 0.04	< 0.04	0.18	0.14	< 0.04		0.07	0.06	0.17	< 0.04	0.04	0.12	0.22
Al_2O_3	< 0.03		5.6	3.4	7.0	3.2	< 0.03		4.1	2.4	5.2	4.9	3.8	5.7	4.4
Cr_2O_3	< 0.05		0.98	0.51	1.22	0.56	< 0.05		1.09	0.45	1.48	0.93	0.62	1.33	0.90
FeO	9.4	0.1	6.3	6.2	2.7	2.6	8.9	0.1	5.8	5.9	2.8	6.4	6.6	3.1	2.9
MnO	0.13	0.01	0.13	0.20	< 0.07	0.10	0.12	0.01	0.13	0.13	0.09	0.13	0.07	< 0.07	0.10
MgO	49.6	0.1	33.2	34.0	15.0	17.2	50.1	0.1	32.5	35.0	16.5	32.6	32.3	16.2	16.9
CaO	< 0.04	0.00	0.98	0.53	24.5	23.7	0.07	0.03	1.33	0.69	20.7	1.30	1.25	22.9	22.6
Na_2O	< 0.04		< 0.04	< 0.04	0.22	0.22	< 0.04		0.04	< 0.04	0.59	< 0.04	< 0.04	0.26	0.32
K_2O	< 0.03		< 0.03	< 0.03	0.03	0.00	< 0.03		< 0.03	< 0.03	< 0.03	< 0.03	< 0.03	< 0.03	< 0.03
NiO	0.37	0.01	n.a.	n.a.	n.a.	n.a.	0.39	0.02	0.10	0.06	0.03	n.a.	n.a.	n.a.	n.a.
total	100.3		101.3	100.8	101.4	100.8	100.8		100.3	101.8	99.8	100.8	99.4	100.2	100.3
Mg#	0.90	0.00	0.90	0.91	0.91	0.92	0.91	0.00	0.91	0.91	0.91	0.90	0.90	0.90	0.91
Cr#			0.11	0.09	0.10	0.10			0.15	0.11	0.16	0.11	0.10	0.14	0.12

Matsumoto *et al.*, 1995; Ahamed *et al.*, 2001, Ahamed & Arai, 2002; Morishita *et al.*, 2006). We find no such direct evidence for hydrous conditions in the formation of our spinel micropods, which appear to be inclusion free.

Chromites in genetically related basalts and mantle peridotites have similar composition ranges (Dick & Bullen, 1984). Despite a data base well over a thousand samples, extremely few peridotites and basalts with chromite with Cr# > 0.6 are reported for *in-situ* ocean crust and mantle, whereas high-Cr# spinel (> 0.7) is commonly found in arc-related magmas (Dick & Bullen, 1984; Arai, 1992, 1994a, b; Robinson, *et al.*, 1997). The Cr# of spinel in the spinel micropods is similar to the lower range of those in mid-ocean ridge basalts collected from around the Atlantis II Transform (Fig. 6). High-Cr magmas, probably related to subduction zone magmatism, then are likely required to form high-Cr chromitites. This study suggests that local concentration of spinel can be found in every geodynamic settings, but economically important large high-Cr chromite deposits appear to be restricted to supra-subduction zone settings.

Conclusions

We present the first detailed petrology and mineralogy of a local concentration of spinel from the slow-spreading Southwest Indian Ridge. Spinel is locally concentrated in small pods with centimeter scale in spinel-poor dunite associated with an enstatite-poor harzburgite host occurring in an outcrop area largely dominated by spinel lherzolite. Petrographical and mineralogical data suggest that the Enstatite-poor harzburige is a residue of mantle melting with subsequent crystallization of clinopyroxene from infiltrating interstitial melts. The Cr# of spinel in the spinel micropods is lower than in typical podiform chromitites from ophiolites and orogenic peridotites. Studies of REE and major element chemistry of MORB in the Atlantis II Fracture Zone region show that these were produced by relatively low degree of mantle melting (Robinson *et al.*, 1996). The low Cr# of spinel in the spinel micropods in this study, which is similar to that in some MORB's, then, likely reflects the geochemical characteristics of mid-ocean ridge basalts derived by this low-degree of partial melting. The spinel micropods were formed as a result of melt-peridotite interactions. This study suggests that local concentration of spinel occurs in every geodynamic settings, but economically important chromite are likely restricted to supra-subduction zone where both moderately depleted peridotite and high-Cr magmas are expected to be coexisting.

Acknowledgements: We are grateful to Captain Ishida and the crew of the Yokosuka and the Shinkai Team who contributed to the success of the cruise. We also thank M. Cheadle, B. John, Y. Otomo, A. Kavassnes, G. Baines, A. Hamadate, M. Imamura, E. Miranda and J. Warren, for their help in collecting the data and discussions on board. T.M. deeply thanks S. Arai for his daily discussions on origin of chromitites. The manuscript was improved by valuable comments from Marja Lehtonen and three anonymous reviewers. This study is partly supported by a Grant-in-Aid for Scientific Research of the Ministry of Education, Culture, Sports, Science and Technology of Japan (No. 17740349) to T.M.

References

Abe, N. & ODP Leg 209 Scientific Party (2003): Petrological insights of the first recovered chromitites from Site 1271, ODP Leg 209, MAR 15N. *EOS Trans. AGU abst.*, **84**, V11E-0533.

Ahmed, A.H. & Arai, S. (2002): Unexpectedly high-PGE chromitite from the deeper mantle section of the northern Oman ophiolite and its tectonic implications. *Contrib. Mineral. Petrol.*, **143**, 263-278.

Ahmed, A.H., Arai, S., Attia, A.K. (2001): Petrological characteristics of podiform chromitites and associated peridotites of the Pan African Proterozoic ophiolite complexes of Egypt. *Mineral. Dep.,* **36**, 72-84.

Andal, E.S., Arai, S., Yumul, G.P. Jr. (2005): Complete mantle section of a slow spreading ridge-derived ophiolite: an example from the Isabela Ophiolite (Philippines). *The Island Arc*, **14,** 272-294.

Arai, S. (1978): A massive chromitite nodule in alkali olivine basalt from Takashima, Southwestern Japan. *Rep. Fac. Sci., Shizuoka Univ.*, **12**, 99-113.

— (1987): An estimation of the least depleted spinel peridoittes on the basis of olivine-spinel mantle array. *Neues Jahrb. Mineral. Mh.*, **1987**, 347-357.
— (1992): Chemistry of chromian spinel in volcanic rocks as a potential guide to magma chemistry. *Mineral. Mag.*, **56**, 173-184.
— (1994a): Characterization of spinel peridotites by olivine-spinel compositional relationships: review and interpretation. *Chem. Geol.*, **113**, 191-204.
— (1994b): Compositional variation of olivine-chromian spinel in Mg-rich magmas as a guide to their residual spinel peridotites. *J. Vol. Geotherm. Res.*, **59**, 279-293.
— (1995): Possible sub-arc origin of podiform chromitites. *The Island Arc* **4**, 104-111.
— (1997a): Control of wall-rock composition on the formation of podiform chromitites as a result of magma/peridotite interaction. *Res. Geol.*, **47**, 177-187.
— (1997b): Origin of podiform chromitites. *J. Asian Earth Sci.*, **15**, 303-310.
— (1998): Comments of the paper "Primitive basaltic melts included in podiform chromites from the Oman ophiolite" by P. Schiano et al. *Earth Planet. Sci. Lett.*, **156**, 117-119.
Arai, S. & Abe, N. (1994): Podiform chromitite in the arc mantle: chromitite xenoliths from the Takashima alkali basalt, Southwest Japan arc. *Mineral. Dep.*, **29**, 434-438.
—, — (1995): Reaction of orthopyroxene in peridotite xenoliths with alkali-basalt melt and its implication for genesis of alpine-type chromitite. *Amer. Mineral.*, **80**, 1041-1047.
Arai, S. & Matsukage, K. (1998): Petrology of a chromitite micropod from Hess Deep, equatorial Pacific: a comparison between abyssal and alpine-type podiform chromitites. *Lithos* **43**, 1-14.
Arai, S. & Yurimoto, H. (1994): Podiform chromitites of the Tari-Misaka ultramafic complex, southwestern Japan, as mantle-melt interaction products. *Econ. Geol.*, **89**, 1279-1288.
Augé, T. (1987): Chromite deposits in the northern Oman ophiolite: mineralogical constraints. *Mineral. Dep.*, **22**, 1-10.
Bloomer, S.H., Natland, J.H., Fisher, R.L. (1989): Mineral relationships in gabbroic rocks from fracture zones of Indian Ocean ridges: evidence for extensive fractionation, parental diversity and boundary-layer recystallization, *in* "Magmatism of Ocean Basins" , A.D. Saunders & M. J. Norry eds. Geological Society Special Publication, no. 42, 107-124.
Boudier, F. & Nicolas, A. (1985): Harzburgite and Lherzolite subtypes in ophiolitic and oceanic environments. *Earth Planet. Sci. Lett.*, **76**, 84-92.
Campbell, I.H. & Murck, B.W. (1993): Petrology of the G and H chromitite zones in the Mountain View area of the Stillwater Complex, Montana. *J. Petrol.*, **34**, 291-316.
Dick, H.J.B. (1974): The Josephine Peridotite, a refractory residue of the generation of andesite. EOS, Am. Geoph. Union, **56**, 464.
— (1976): Origin and emplacement of the Josephine Peridotite of southwestern Oregon. Ph D Thesis, Yale University, 409 pp.
— (1977a): Partial melting in the Josephine Peridotite I, the effect on mineral composition and its consequence for geobarometry and geothermometry. *Amer. J. Sci.*, **277**, 801-832.
— (1977b): Evidence for partial melting in the Josephine Peridotite. *Ore Dept. Geol. Min. Ind. Bull.*, **96**, 59-62.
— (1989): Abyssal peridotites, very slow spreading ridges and ocean ridge magmatism. *in* "Magmatism of Ocean Basins", A.D. Saunders & M.J. Norry eds. Geological Society Special Publication no. 42, 71-105.
Dick, H.J.B. & Bullen, T. (1984): Chromian spienl as a petrogenetic indicator in abyssal and alpine-type peridotites and spatially associated lavas. *Contrib. Mineral. Petorol.*, **86**, 54-76.
Dick, H.J.B. & Sinton, J. (1979): Compositional layering in alpine peridotites: evidence for pressure solution creep in the mantle. *J. Geol.*, **87**, 403-416.
Dick, H.J.B. & Natland, J.H. (1996): Last stage melt evolution and transport in the shallow mantle beneath the East Pacific Rise. *Proc. ODP, Sci. Res.*, **147**, 103-134.
Dick, H.J.B., Natland, J.H., Alt, J.C., Bach, W., Bideau, D., Gee J.S., Haggas, S., Hertogen, J.G.H., Hirth, G., Holm, P.M., Ildefonse, B., Iturrino, G.J., John, B. E, Kelley, D.S., Kikawa, E., Kingdon, A., LeRux, P.J., Maeda, J., Meyer, P. S., Miller, D.J., Naslund, H.R., Niu, Y-L., Robinson, P.T., Snow, J., Stephen R.A., Trimby, P.W., Worm H-U., Yoshinobu A. (2000): A long in situ section of the lower ocean crust: results of ODP Leg 176 drilling at the Southwest Indian Ridge. *Earth Planet. Sci. Lett.*, **179**, 31-51.
Edwards, S.J., Pearce, J.A., Freeman J. (2000): New insights concerning the influence of water during the formation of podiform chromitite. *in* "Ophiolites and Oceanic Crust: New insights from Field Studied and the Ocean Drilling program", Y., Dillek, Moores E.M., Elthon, E. m., Nicolas, A. eds.. Geological Society Special Publication no. 349, 139-147.
Gervilla, F. & Leblanc M. (1990): Magmatic ores in high-temperature alpine-type lherzolite massifs (Ronda, Spain, and Beni Bousera, Morocco). *Econ. Geol.*, **85**, 112-132.
Hellebrand, E., Snow, J.E., Mübe, R. (2002): Mantle melting beneath Gakkel Ridge (Arctic Ocean): abyssal peridotite spinel compositions. *Chem. Geol.*, **182**, 227-235.
Hellebrand, E., Snow, J.E., Mübe, R., J.E., Dick, H.J.B., Hofmann, A.W. (2001): Coupled major and trace elements as indicators of the extent of melting in mid-ocean-ridge peridotites. *Nature*, **410**, 677-681.
Hosford, A., Tivey, M., Matsumoto, T., Dick, H.J.B., Schouten, H., Kinoshita, H. (2003): Crustal magnetization and accretion at the Southwest Indian Ridge near the Atlantis II fracture zone, 0-25Ma. *J. Geophys. Res.*, **108,** 2169-2191.
Johan, Z., Dunlop, H., Le Bel, L., Robert, J.L., Volfinger, M. (1980): Origin of chromite deposits in ophiolitic complexes: evidence for a volatile- and sodium-rich reducing fluid phase. *Fortsch. Mineral.*, **61**, 105-107.
Johnson, K.T.M. & Dick, H.J.B. (1992): Open system melting and temporal and spatial variation of peridotite and basalt at the Atlantis II Fracture Zone. *J. Geophys. Res.*, **97**, 9219-9241.
Kelemen, P.B. (1990): Reaction between ultramafic rocks and fractionating basaltic magma I. Phase relathions, the origin of calc-alkaline magma series, and the formation of dicordant dunite. *J. Petrol.,* **31**, 51-98.
Irvine, T.N. (1975): Crystallization sequences in the Muskox intrusion and other layered intrusions – II. Origin of chromitite layers and similar deposits of other magmatic ores. *Geochim. Cosmochim. Acta*, **39**, 991-1020.
— (1977) Oriign of chromitite layers in the Muskox intrusion and other stratiform intrusions: A new interpretation. *Geology*, **5**, 273-277.
Lago, B.L., Rabinowicz, M., Nicolas, A. (1982): Podiform chromite ore bodies: a genetic model. *J. Petrol.*, **23**, 103-125.
Leblanc, M. & Ceuleneer, G. (1992): Chromite crystallization in a multicellular magma flow: evidence from a chromitite dike in the Oman ophiolite. *Lithos*, **27**, 231-257.
Leblanc, M., Ceuleneer, G., Temagoult, A. (1989): Chromite pods in a lherzolite massif (Collo, Algeria): evidence of oceanic-type mantle rocks along the West Mediterranean Alpine Belt. *Lithos* **23**, 153-162.
le Roex, A.P., Dick, H.J.B., Erlank, A.J., Reid, A.M., Frey F.A., Hart, S.R. (1983): Geochemistry, mineralogy and petrogenesis

of lavas erupted along the Southwest Indian Ridge between the Bouvet Triple Junction and 11 degrees East. *J. Petrol.*, **24**, 267-318.

Lorand, J.P. & Ceuleneer, G. (1989): Silicate and base-metal sulfide inclusions in chromites from the Maqsad area (Oman ophiolite, Gulf of Oman): a model for entrapment. *Lithos*, **22**, 173-190.

Matsukage, K. & Arai, S. (1998): Jadeite, albite and nepheline as inclusions in spinel of chromitite from Hess Deep, equatorial Pacific: their genesis and implications for serpentinite diapir formation. *Contrib. Mineral. Petrol.*, **131**, 111-122.

Matsumoto, I., Arai, S., Harada, T. (1995): Hydrous mineral inclusions in chromian spinel from the Yanaomine ultramafic complex of the Sangun zone, Southwest Japan. *J. Mineral. Petrol. Econ. Geol.,* **90**, 333-338. (in Japanese with English abstract)

McElduff, B. & Stumpfl, E.F. (1991) The chromite deposits of the Troodos Complex, Cyprus-evidence for the role of a fluid phase accompanying chromite formation. *Mineral. Dep.*, **26**, 307-318.

Morishita, T., Maeda, J., Miyashita, S., Matsumoto, T., Dick, H.J. (2004): Magmatic srilankite (Ti_2ZrO_6) in gabbroic vein cutting oceanic peridotites: an unusual product of peridotite-melt interactions beneath slow-spreading ridges. *Amer. Mineral.*, **89**, 759-766.

Morishita, T., Andal, E.S., Arai, S., Ishida, Y. (2006): Podiform chromitites in lherzolite-dominant mantle section of the Isabela ophiolite, Philippines. *The Island Arc*, **15**, 84-101.

Nicolas, A. (1992): *Structures in Ophiolites and Dynamics of Oceanic Lithosphere*, Kluwer Academic Publishers, Dordrecht, 367 p.

Nicolas, A. & Al Azri, H. (1991): Chromite-rich and chromite-poor ophiolites: The Oman Case. *in* "Ophiolite Genesis and Evolution of the Oceanic Lithosphere" T. J., Peters, A., Nicolas & R.G., Coleman. eds. Kluwer, Dordrecht, the Netherlands, 261-274.

Noller, J.S. & Carter, B. (1986): The origin of various types of chromite schlieren in the Trinity Peridotite, Klamath Mountains, California. *in* "Metallogeny of Basic and Ultrabasic Rocks (Regional Presentations)" B., Carter, M.K.R., Chowdhury., S., Jankovic, A.A., Marakushev, L., Morten, V.V., Onikhimovsky, G., Raade, G., Rocci, S.S., Augstithis. eds. Theophrastus, Athens, Greece, 151-178.

Piccardo, G.B., Zanetti, A., Müntener, O. (2007): Melt/peridotite interaction in the Southern Lanzo peridotite: filed, textural and geochemical evidence. *Lithos* **94**, 181-209.

Prichard, H.M., Lord, R.A., Neary, C.R. (1996): A model to explain the occurrence of platinum- and palladium-rich ophiolite complexes. *J. Geol. Soc. London*, **153**, 323-328.

Quick, J.E. (1981): The origin and significance of large, tabular dunite bodies in the Trinity Peridotite, northern California. *Contrib. Mineral. Petrol.*, **78**, 413-422.

Roberts, S. (1988): Ophiolitic chromitite formation: a marginal basin phenomenon? *Econ. Geol.*, **83,** 1034-1036.

Roberts, S. & Neary, C. (1993): Petrogenesis of ophiolitic chromitite. *in* "Magmatic Processes and Plate Tectonics", H.M., Prichard, T., Alabaster, N.B.W., C.R., Neary eds.. Geological Society Special Publication no. 76, 257-272.

Roeder, P.L. & Reynolds, I. (1991): Crystallization of chromite and chromium solubility in basaltic melts. *J. Petrol.*, **32**, 909-934.

Robinson, P.T., Zhou, M.F., Malpas, J., Bai. W-J. (1997): Podiform chromitites: their composition, origin and environment of formation. *Episodes* **20**, 247-252.

Schiano, P., Clocchiatti R., Lorand, J.–P., Massare, D., Deloule, E., Chaussidon, M. (1997): Primitive basaltic melts included in podiform chromites from the Oman Ophiolite. *Earth Planet. Sci. Lett.,* **146**, 489-497.

Seyler, M., Toplis, M.J., Lorand, J-P., Luguet, A., Cannat, M. (2001): Clinopyroxene microtexture reveal incompletely extracted melts in abyssal peridotites. *Geology,* **29**, 155-158.

Sobolev, A.V. & Shimizu, N. (1993): Ultra-depleted primary melt included in an olivine from the Mid-Atlantic Ridge. *Nature*, **363**, 151-154.

Talkington, R.W., Watkinson, D.H., Whittaker, P.J., Jones, P.C. (1986): Platinum group element-bearing minerals and other solid inclusions in chromite of mafic and ultramafic complexes: chemical compositions and comparisons. *in* "Metallogeny of Basic and Ultrabasic Rocks (Regional Presentations)" B., Carter, M.K.R., Chowdhury., S., Jankovic, A.A., Marakushev, L., Morten, V.V., Onikhimovsky, G., Raade, G., Rocci, and S. S., Augstithis. eds. Theophrastus, Athens, Greece, 223-249.

Thayer, T.P. (1964): Principal features and origin of podiform chromite deposits, and some observations on the Guleman-Soridag district, Turkey. *Econ. Geol.*, **59**, 1497-1524.

Toramaru, A. & Fujii, N. (1986): Connectivity of melt phase in a partially molten peridotite. *J. Geophys. Res.*, **91**, 9239-9252.

Yumul, G.P. Jr. (1992): Ophiolite-hosted chromitite deposits as tectonic setting and melting degree indicators: examples from the Zambales Ophiolite Complex, Luzon, Philippines. *Min. Geol.*, **42**, 5-17.

Zhou, M.-F. & Robinson, P.T. (1997): Origin and tectonic environment of podiform chromite deposits. *Econ. Geol.*, **92**, 259-262.

Zhou, M.-F., Robinson, P.T., Bai, W. –J. (1994): Formation of podiform chromitites by melt/rock interaction in the upper mantle. *Mineral. Dep.*, **29**, 98-101.

Zhou, M.-F., Robinson, Malpas, J., Li, Z. (1996): Podiform chromitites in the Lubusa ophiolite (southern Tibet): implications for melt-rock interaction and chromite segregation in the upper mantle. *J. Petrol.*, **37**, 3-21.

Zhou, M.-F., Robinson, Sun., M., Keays, R.R., Kerrich, R.W. (1998). Controls on platinum-group elemental distributions of podiform chromitites: a case study of high-Cr and high-Al chromitites from Chinese orogenic belts. *Geochim. Cosmochim. Acta*, **62**, 677-688.

Zhu, W. & Hirth, G. (2003): A network model for permeability in partially molten rocks. *Earth Planet. Sci. Lett.*, **212**, 407-416.

Received 3 December 2006
Modified version received 28 August 2007
Accepted 3 September 2007